



Rit Veðurstofu Íslands

*Sigurður Th. Rögnvaldsson
Ágúst Guðmundsson
Ragnar Slunga*

*Seismotectonic analysis of the
Tjörnes fracture zone - an active
transform fault in North Iceland*

VÍ-R98004-JA03
Reykjavík
September 1998

ISSN 1025-0565
ISBN 9979-878-11-8

*Sigurður Th. Rögnvaldsson
Ágúst Guðmundsson
Ragnar Slunga*

*Seismotectonic analysis of the
Tjörnes fracture zone - an active
transform fault in North Iceland*

VÍ-R98004-JA03
Reykjavík
September 1998

CONTENTS

1	SUMMARY	5
2	INTRODUCTION	5
3	METHODS	7
4	THE MICROEARTHQUAKE DATA	8
5	EXAMPLES	10
6	THE GRÍMSEY LINEAMENT	13
7	THE HÚSAVÍK-FLATEY FAULT	15
8	THE DALVÍK LINEAMENT	18
9	DISCUSSION AND CONCLUSIONS	19
10	REFERENCES	21



1 SUMMARY

The Tjörnes fracture zone is a transform fault connecting the rift zone of the Kolbeinsey ridge with that of North Iceland. The main transform motion takes place on the Húsavík-Flatey fault, a major 7–9 million years old right-lateral fault. In addition to this fault, there are two major seismic lineaments associated with the Tjörnes fracture zone; the Grímsey lineament and the Dalvík lineament. These lineaments are marked by concentrations of seismicity with the largest earthquakes reaching magnitude 7. The maximum depth of earthquakes is 10–12 km and increases with distance from the spreading axis. We determined accurate relative locations and focal mechanisms of more than 800 earthquakes in 62 clusters on the principal seismic lineaments. The estimated relative location uncertainty for most of the relocated earthquakes is 2–20 m. The best-fitting plane through each cluster is assumed to coincide with the fault plane of the group of earthquakes. For clusters near the Húsavík-Flatey fault the fault planes are right-lateral and strike N122°E–N140°E, similar to the overall strike of the Húsavík-Flatey fault. This agrees with the right-lateral displacement on the fault as well as with field observations of numerous transform-parallel right-lateral faults associated with the main fault. By contrast, earthquake clusters on the lineaments of Grímsey and Dalvík define (mostly) left-lateral planes striking roughly N-S, i.e. at 40°–90° to the overall trend of these lineaments. Field observations show that left-lateral, north-south trending fault planes are also common in the on-land parts of the Dalvík lineament. The different style of faulting probably represents transform faults at different stages of development.

2 INTRODUCTION

Most of the seismicity in North Iceland is associated with the Tjörnes fracture zone (TFZ), a transform fault connecting the rift zone in North Iceland with that of the Kolbeinsey ridge (Figure 1). The seismicity of the Tjörnes fracture zone occurs in a WNW-trending zone that is roughly 120 km long (E-W) and as much as 70 km wide (N-S). The earthquake epicenters define two main WNW-trending seismic lineaments; the Grímsey lineament and the Húsavík-Flatey fault (HFF). There is also an indication of a third lineament south of the HFF, the Dalvík lineament.

The Húsavík-Flatey fault is the main structure of the Tjörnes fracture zone and should be identified with the transform-tectonized zone of a normal oceanic fracture zone (Fox and Gallo 1986). The HFF is partly exposed on land on the peninsulas of Tjörnes and Flateyjarskagi (Figure 1), where its infrastructure can be studied in great detail (Jancin et al. 1985; Guðmundsson et al. 1993; Fjäder et al. 1994). Offshore Flateyjarskagi there is a 3–4 km deep graben running parallel with the fault (Flóvenz and Gunnarsson 1991). This graben is partly filled with sediments and gives rise to a pronounced negative Bouguer gravity anomaly. Other main features of the TFZ include several N-S trending grabens, presumably related to previous and current locations of the rift zone in North Iceland (Sæmundsson 1974, 1979; McMaster et al. 1977).

The TFZ is seismically very active. In 1872, a major earthquake sequence, with the two largest earthquakes reaching $M = 6.3$, occurred on the Húsavík-Flatey fault, causing severe damage in the village of Húsavík and on the island of Flatey (Figure 1 and Figure 7). In 1910, a $M = 7.1$ earthquake occurred on the Grímsey lineament (Tryggvason 1973) and a $M = 6.4$ earthquake in 1976 near its eastern end (Einarsson 1987). In 1963 a $M = 7$ earthquake occurred off-shore in the southwestern part of the TFZ (Stefánsson 1966), and in 1934 several buildings were damaged

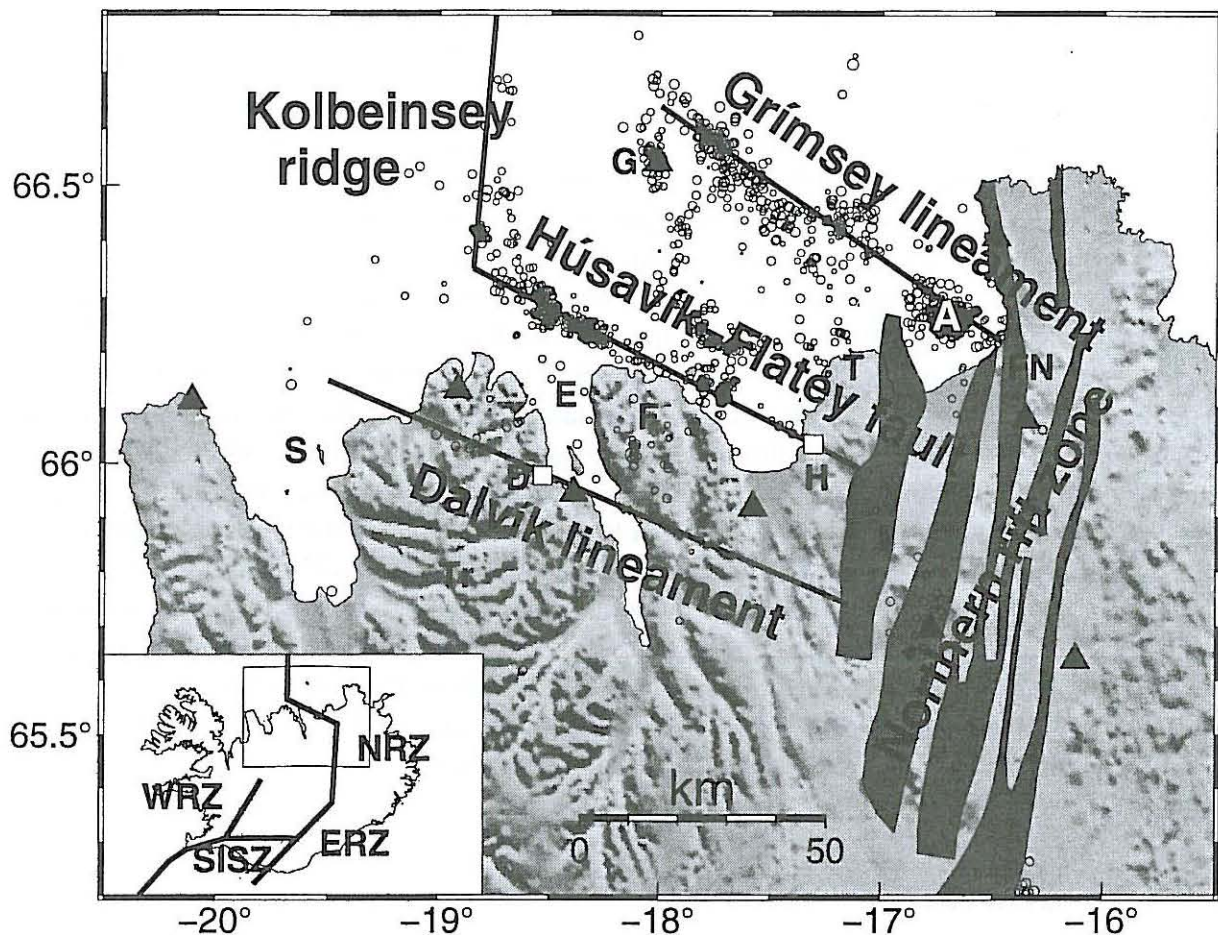


Figure 1. The Tjörnes fracture zone. The main tectonic features, the Kolbeinsey ridge, Húsavík-Flatey fault and the Grímsey and Dalvík lineaments, are shown schematically as black lines on the map. Earthquake epicenters are shown as circles. S, E and A are the fjords Skagafjörður, Eyjafjörður and Axarfjörður. Tr, F and T are the Tröllaskagi, Flateyjarskagi and Tjörnes peninsulas, G is Grímsey island and FN is the Fremri-Námar volcanic system. White boxes indicate the towns Dalvík (D) and Húsavík (H). The inset is a schematic overview of the plate boundaries in Iceland. The western, eastern and northern rift zones are denoted WRZ, ERZ and NRZ, respectively. SISZ is the South Iceland seismic zone. The box outlines the Tjörnes fracture zone in North Iceland.

in a $M = 6.3$ earthquake on the Dalvík lineament.

A $M = 5.5$ earthquake at the junction between the TFZ and the Kolbeinsey ridge in February 1994 was followed by intense activity at the western end of the Húsavík-Flatey fault and the southernmost part of the Kolbeinsey ridge for a few weeks. From July 1997, when a $M = 4.5$ earthquake occurred on the western end of the HFF, until October 1997, activity has continued there with varying intensity. The largest earthquakes of that swarm were two $M = 5$ strike-slip events in September 1997. Small earthquake swarms are common in the TFZ but mainshock-aftershock sequences, where the mainshock is much larger than the other events, are rare.

We analyzed more than 60 earthquake swarms recorded during the period 1994–1998. By cross-correlating waveforms of similar earthquakes in a swarm, we obtain highly accurate arrival time

differences which are used to constrain the relative and absolute locations of the earthquakes. Accurate relative locations of earthquakes can be used to map the fault planes on which the earthquakes occurred (Slunga et al. 1984; Rögnvaldsson and Slunga 1994; Slunga et al. 1995). The determination of the attitude and sense of slip on active faults can then be compared with field observations of similar faults exposed in the on-land parts of the Tjörnes fracture zone.

The principal objective of this paper is to present a detailed seismotectonic analysis of the Tjörnes fracture zone in general and the Húsavík-Flatey fault in particular. This is done by comparing the seismically determined parameters of the currently active faults with the parameters obtained from field measurements in the on-land parts of the fracture zone. We demonstrate the usefulness of accurate relative locations in determining the type of faulting generating microearthquake clusters. Application of the technique to a large number of earthquake clusters reveals that faulting at the HFF is very different from that in the Grímsey lineament and the Dalvík lineament.

3 METHODS

The shape of the waveforms recorded for an earthquake, at a given station, depends on the hypocenter location, the focal mechanism and the source time function. Earthquakes occurring at nearly the same location (e.g. on the same fault) are therefore likely to generate similar waveforms. The strong similarity often observed between the signals of closely spaced earthquakes recorded at the same station means that signal analysis can give very accurate estimates of the arrival time difference. By cross-correlating waveforms of similar events, arrival time differences can be determined with an accuracy much better than the sampling interval of the digital seismograms. For our data, the timing accuracy is of the order of one millisecond, while the sampling is done at ten millisecond intervals (Böðvarsson et al. 1996; Slunga et al. 1995).

The extreme timing accuracy can be used to determine very accurate relative locations of earthquakes. If similar events originate close to each other, the ray paths for the events will be practically the same. The only difference in travel times is due to the small location differences, as seen from the observing station. The most common approach is to use some variation of the master event method, i.e. to find the absolute location of one earthquake (the master event) using some standard single-event location algorithm. The locations of other similar events, relative to the master event, are then determined by comparing their waveforms to those of the master event (e.g. Deichmann and Garcia-Fernandez 1992; Console and Giovambattista 1987; Ito 1985; Frémont and Malone 1987). Cross-correlating all possible pairs of events, rather than correlating each event with a master earthquake, provides additional constraints on the relative locations (Slunga et al. 1984, 1995; Rögnvaldsson and Slunga 1994; Got et al. 1994).

The timing accuracy achieved by cross-correlation techniques can be used not only to determine relative locations but also to estimate absolute locations. The main sources of error when locating with time differences of similar events are the uncertainties in the ray directions in the source volume. The deviations of ray directions from those predicted by the model are partly independent of the integrated travel time error along the path. This means that the absolute location errors from the use of arrival time differences are nearly independent of the single-event location errors. For most of the groups the estimated standard deviations of the absolute locations are in the range 200–600 m for all three spatial coordinates. This is up to one order of magnitude smaller than the estimated standard deviations of the single-event locations. As the corresponding sizes of the standard deviations of the relative locations are supported by the

deviations from the planes it is plausible that the absolute locations are realistic also. However, differences between the velocity model and true velocity structure can cause location errors exceeding the estimated uncertainties.

Following the method described by Slunga et al. (1995), we simultaneously perform single-event locations, joint hypocenter determination and accurate relative locations for a cluster of similar earthquakes. We retain the absolute formulation of the problem because the high accuracy of the relative timing can then yield extremely accurate relative locations and may also improve the absolute location. This happens if the absolute location significantly affects the theoretical arrival time differences. In our formulation, we put no restrictions on the absolute locations. If the geometry is such that the arrival time differences favor a particular absolute location, the group may move there. In earlier versions of the algorithm, the swarm was considered a single group and all earthquakes of the swarm were located simultaneously. In this study the waveforms for each event are correlated with waveforms for the 10 to 20 nearest neighbors and the earthquake is then located together with the 6 to 12 best correlating events of the cluster. Every event will be included in several subgroups and located once for each of those. After locating all subgroups, a single hypocenter is determined for each earthquake by taking a weighted average of all locations for the event. The weights are based on the approximate error estimates produced by the group analysis (Slunga et al. 1995). Inconsistent estimates are iteratively truncated until a consistent set of absolute locations for each event is achieved. It is required that every event included in the output has been well located in at least two different groups. The purpose of this approach is to increase computational efficiency when working with large swarms.

The waveforms are correlated within a frequency band which is determined by the corner frequency of the event to be correlated with its neighbors. In the correlation procedure the frequency band is restricted to 3–20 Hz; typically 4–12 Hz were used. The correlation of the waveforms is required to be consistent with the correlation of the waveform envelopes. The correlation of the envelopes is less accurate than waveform correlation so the relative timing is based only on the correlation of the waveforms. The check with envelope correlation makes the procedure more robust.

Fault plane solutions were estimated using the P wave polarities and absolute spectral amplitudes of the direct P and S waves. The fault plane solutions are obtained by systematically searching over the entire parameter space for strike, dip and rake and comparing predicted polarities and amplitudes to observations. The output is a range of acceptable solutions, as well as a single best fitting mechanism (Slunga 1981; Rögnvaldsson and Slunga 1993).

4 THE MICROEARTHQUAKE DATA

The earthquakes analyzed here were recorded by a network of digital, 3-component seismic stations connected to a common data center. The data are sampled at 100 Hz, have 136 dB dynamic range and resolution better than 90 dB. The network is an extension of the South Iceland Lowland (SIL) network (Stefánsson et al. 1993; Böðvarsson et al. 1996). The first 6 stations in northern Iceland were installed in December 1993 and 3 additional stations in 1996. From January 1994 through August 1997 the network recorded more than 14000 events within the Tjörnes fracture zone. Most of the seismicity takes place in the offshore parts of the TFZ, whereas the seismic stations are located on land. The theoretical uncertainty in the routinely determined hypocenter locations is therefore commonly ± 2 –10 km, depending both on the

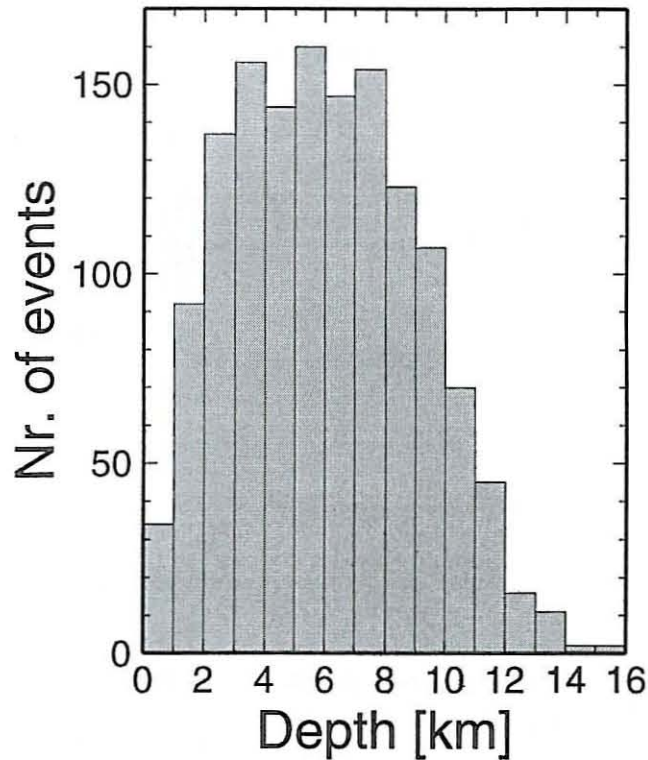


Figure 2. *Depth distribution of 1400 earthquakes in the TFZ relocated with less than ± 1 km estimated horizontal uncertainty and ± 2 km uncertainty in depth. 90% of the earthquakes occur at less than 10 km depth and no earthquakes are located at depths greater than 16 km.*

event location and the number of recording stations.

In the dataset we looked for events clustered in time and space. The selected swarms all lasted less than 96 hours, included at least 6 earthquakes and all events in each swarm were initially located within an area of 20×20 km². We analyzed about 80 groups satisfying these criteria, consisting of a total of more than 3000 earthquakes. Each group was located separately. During the iterative relocation procedure almost half of the events were rejected, leaving nearly 1900 successfully relocated earthquakes. Of these about half belonged to groups where the mean distance of events from the best fitting plane through the group was greater than our ad hoc limit of 50 m. Of the remaining 948 earthquakes 60 were excluded when fitting planes through the groups, leaving 888 events that were used to constrain the orientation of 62 fault planes.

Because of unfavorable station geometry and heterogeneous crustal structure, the single-event locations of earthquakes in the TFZ are often poorly constrained, especially their depths. For events in the same swarms, the initial depth estimates sometimes varied by several kilometers. The arrival time differences used in the location procedure are weighted with distance between events. Thus, if two earthquakes are widely separated due to initial (single-event) location errors, the relative timing data will be down-weighted and have little effect on their final location. The solution obtained will be essentially a joint hypocentral determination for the group. However, the location procedure is not sensitive to the initial depth of a group of similar events, as long as all events of the group have approximately the same starting depths.

Figure 2 shows the depth distribution of the 1400 events relocated with less than ± 2 km absolute

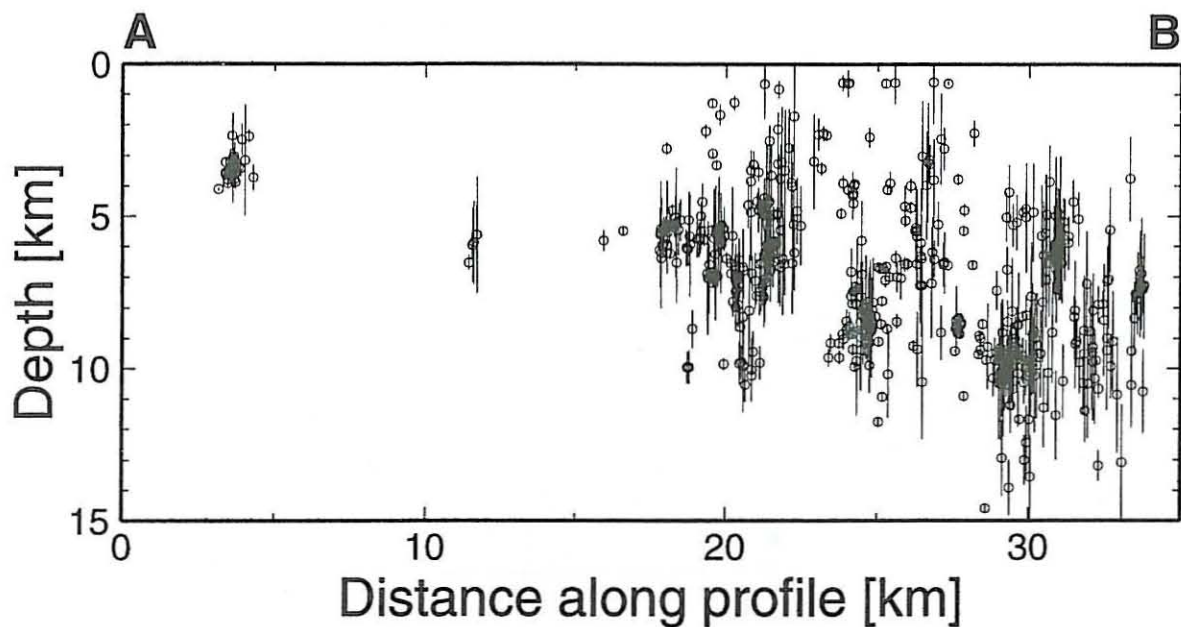


Figure 3. *Depth of earthquakes along a profile parallel to the HFF. The profile location is shown in Figure 7. The open circles are the depths of 596 well located (less than ± 1 km horizontal and ± 2 km vertical uncertainty) events. The vertical bars are the estimated uncertainties in depth after relocation. The maximum depth of earthquakes increases from about 5–6 km near the ridge (point A on the profile) to approximately 11 km at a distance of 30 km.*

uncertainty in depth. Most of the earthquakes occur between 2 and 10 km depth and no events occur below 16 km. Taking the depth above which 90% of the events occur as the depth to the base of the brittle crust gives a depth of about 10 km. The geothermal gradient in shallow boreholes in the on-land parts of the TFZ is approximately $60^{\circ}\text{C}/\text{km}$ (Ólafur G. Flóvenz 1998, pers. comm.) Accordingly a depth of 10 km corresponds to roughly 600°C . This is similar to results in South Iceland where the base of the brittle crust, estimated as the depth to the 90 percentile event at a number of locations, closely follows the inferred 600°C isothermal surface (Tryggvason 1998).

The maximum depth of earthquakes near the western end of the HFF increases with distance from the crust-generating ridge (Figure 3). Earthquakes located near the intersection of the HFF and the southward extension of the Kolbeinsey ridge, the Eyjafjarðaráll graben, occur only in the uppermost 5–6 km while at a distance of 30 km the maximum depth of faulting is about 11 km. This is similar to the observed variation in the maximum depth of earthquakes in South Iceland with distance from the spreading axis. The maximum depth of earthquakes in the SISZ increases from about 6–7 km in young crust near the WVZ to about 13–14 km in older crust at the zone's eastern end (Stefánsson et al. 1993). We note, however, that most of the data in Figure 3 were collected during an unusually active period of less than 3 months. It is possible that the trend seen in Figure 3 reflects temporal rather than spatial variations in the seismicity.

5 EXAMPLES

Estimated uncertainty in longitude, latitude and depth relative to a neighboring event for the 948 events belonging to groups used to estimate fault orientations in the TFZ is shown in Figure 4.

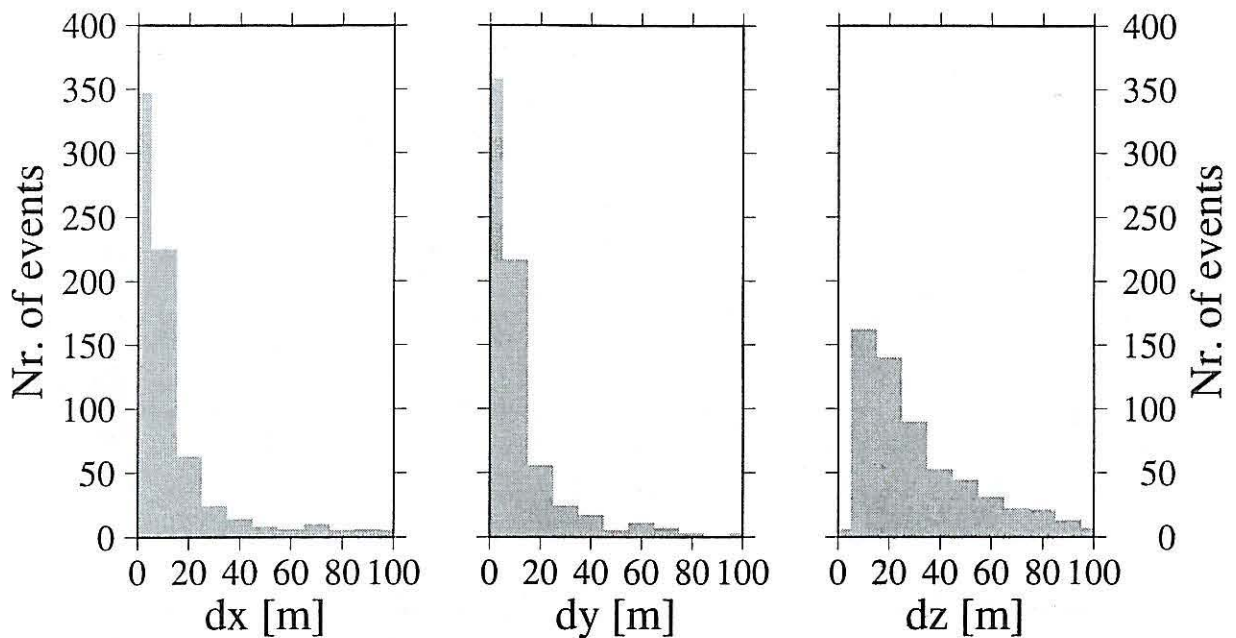


Figure 4. *Relative location uncertainty for 912 earthquakes used to determine fault orientations in the Tjörnes fracture zone. dx , dy and dz are estimated relative uncertainties in longitude, latitude and depth, respectively. Approximately 80% of the events are located with less than ± 100 m relative horizontal location uncertainty and about 70% of the events are located with less than ± 100 m uncertainty in depth, relative to a neighboring event.*

The uncertainty in the relative locations is less than 100 m for approximately 80% of the events and less than 20 m horizontally for 70% of the events. Vertical uncertainty is somewhat greater. Relative horizontal and vertical uncertainty is less than 100 m for approximately 50% of the successfully relocated earthquakes.

Figure 5 shows the results of relocating a group of 55 events just west of the island of Grímsey, at location 1 in Figure 7. During the iterative location procedure 11 events are rejected. Of the successfully located events, 36 form the tight cluster shown in Figure 5. The other 8 are located at distances of more than a kilometer from the line of epicenters and not included in the figure. When determining the best fitting plane through the hypocenters, three more events were excluded. The strike of the best fitting plane is N6°E and its dip is 89°. The mean distance of the 33 earthquakes from the plane is 20 m, comparable to the uncertainty in the relative locations. The normals to all planes with mean distance less than 50 m are shown in Figure 5c on an equal area projection of the lower hemisphere. Clearly the acceptable (according to our definition) plane orientations are confined to a narrow range (approximately $\pm 15^\circ$ in strike and $\pm 25^\circ$ in dip) around the optimal orientation. The earthquake locations can not determine whether the fault dips to the east or west.

A second example is given in Figure 6. This group of events occurred north of the fjord Eyjafjörður at location 2 in Figure 7, near the junction between the Húsavík-Flatey fault and the Kolbeinsey ridge. Initially, the location procedure included 39 earthquakes but four were rejected in the iterative consistency checks. Of the remaining 35 events, 31 form the cluster shown in mapview in Figure 6a and were used to determine a common fault plane for the group. The four events not shown in the figure were located at distance between one and three kilome-

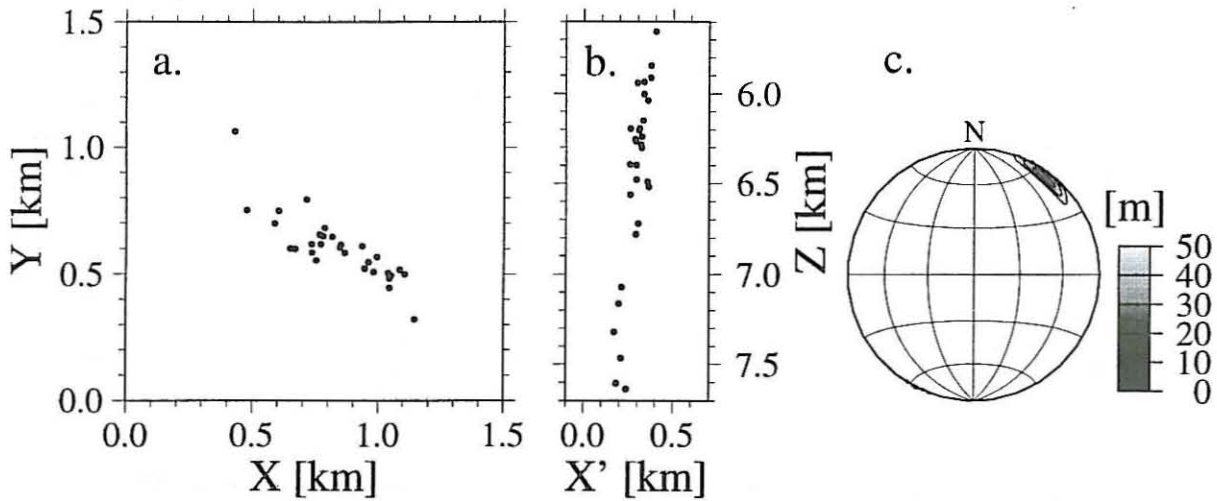


Figure 5. *The relative locations of a cluster of 36 earthquakes after relocation. The cluster is located just west of the island of Grímsey and labelled as 1 in Figure 7. a) A mapview of the epicenter distribution, X is east, Y is north. Events marked with crosses were not used when determining the best fitting plane through the hypocenters. The strike of the best fitting plane is 6° , the dip is 89° and the mean distance of the 33 events from the plane is 20 m. b) View along the strike of the best fitting plane. The horizontal axis is orthogonal to the strike, Z is depth. c) An equal area, lower hemisphere projection of poles to all planes such that the mean distance of the 33 events is less than 50 m.*

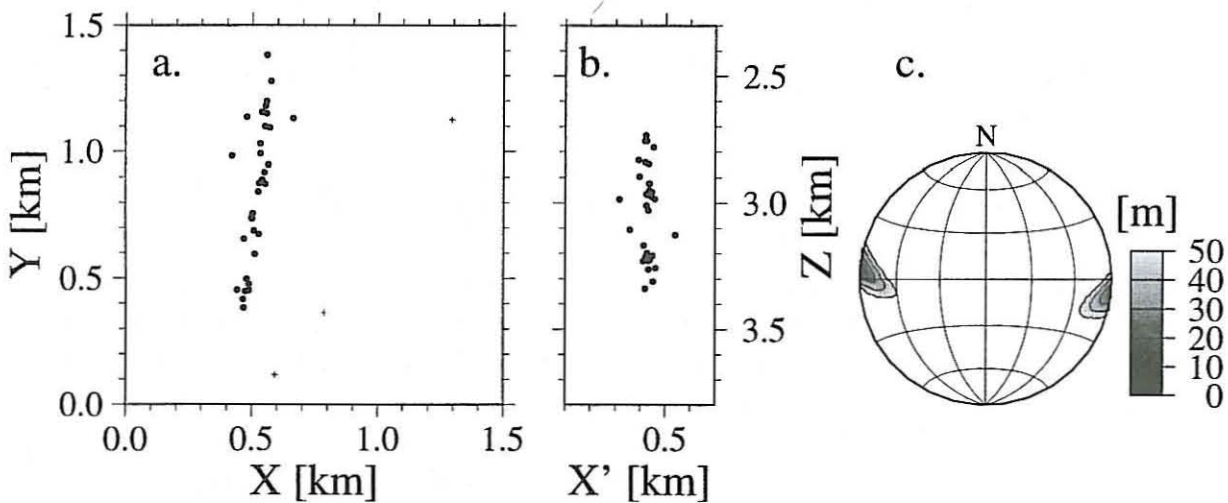


Figure 6. *The relative locations of a cluster of 31 earthquakes after relocation. The location of the group is labelled 2 in Figure 7. a) A mapview of the epicenter distribution, X is east, Y is north. The strike of the best fitting plane is 126° , the dip is 85° and the mean distance of the 33 events from the plane is 25 m. b) View along the strike of the best fitting plane. The horizontal axis is orthogonal to the strike, Z is depth. c) An equal area, lower hemisphere projection of poles to all planes such that the mean distance of the 31 events is less than 50 m.*

ters from the main group. The best fitting plane strikes N126°E and dips 85° to the southwest. The mean distance of the 31 earthquakes from the best fitting plane is 25 m. A plot of normals to possible planes (Figure 6c) shows that acceptable orientations are confined to within approximately $\pm 15^\circ$ from the optimal strike and $\pm 10^\circ$ from optimal dip.

How well the relative locations of a group of earthquakes constrain the orientation of a plane depends mostly on the maximum distance between any two events of the group. Earthquakes in a very dense cluster can not constrain the plane orientation, even if the mean distance from the plane is small. If the earthquakes have narrow depth distribution, the dip of the best fitting plane will be poorly constrained and when the lateral distribution is small, the estimated strike will be poorly determined. The two examples shown in Figures 5 and 6 are fairly representative of the data we have used to estimate fault orientations in the TFZ. A set of Figures like 5 and 6 for all clusters used to determine fault orientations in the TFZ can be viewed on the Web at <http://www.vedur.is/~sr/faults.html>.

6 THE GRÍMSEY LINEAMENT

North of the Húsavík-Flatey fault, earthquake epicenters define a lineament trending approximately N128°E, the Grímsey lineament (Figure 1). Although the seismicity associated with the Grímsey lineament has a clear WNW trend, most of the off-shore structures trend NNW. These are mainly normal faults, some of which form 5–20 km wide grabens, running parallel with the on-land trend of the northernmost part of the fissure swarm of the Fremri-Námar volcanic system (Figure 1). On meeting the Grímsey lineament, the tension fractures and normal faults associated with this volcanic system abruptly change their strike. South of the junction the mode of the fracture-frequency distribution is at N2°W, but north of the junction it changes to N20°W (Guðmundsson et al. 1993). This change in fracture trend at the junction is clearly related to the stress field influence of the TFZ in general and to that of the Grímsey lineament in particular. Apart from this change in trend of the fractures of the Fremri-Námar volcanic system, there is no clear on-land effect of the Grímsey lineament and no major WNW-trending faults occur east of the lineament that could be interpreted as its structural continuation.

We have analyzed 21 swarms of microearthquakes that occurred on or near the Grímsey lineament during 1994–1997 to obtain 25 estimates of fault orientations. After relocation, the earthquakes align on a number of N-S zones, arranged en-echelon along the lineament. The earthquake clusters define steeply dipping (70°–90°) planes, striking roughly north-south (mean direction $14^\circ \pm 14^\circ$), i.e. at approximately 70° to the overall trend of the seismic lineament. The mean distance from best fitting planes varies between 2 and 40 m. To display the results of the accurate relocation procedure and subsequent estimates of fault attitudes, the estimated strike directions are marked in red on the map in Figure 7. The locations and orientations of faults mapped using relative earthquake locations can then be compared with faults mapped with conventional reflection seismic techniques, drawn in black in Figure 7. On most of the N-S planes within the Grímsey lineament, faulting is left-lateral strike-slip with considerable dip-slip component.

Clusters of microearthquakes occur frequently in the fjord Axarfjörður (A in Figure 1), at the SE end of the Grímsey lineament. Of the 10 estimated fault directions in this part of the lineament all but one strike between 19° and 42°. Most fault-plane solutions show strike-slip with either reverse or normal faulting components. If the N-S planes are taken as fault planes, the strike-slip movement is left-lateral. During the first rifting event of the 1975–1984 Krafla episode, a

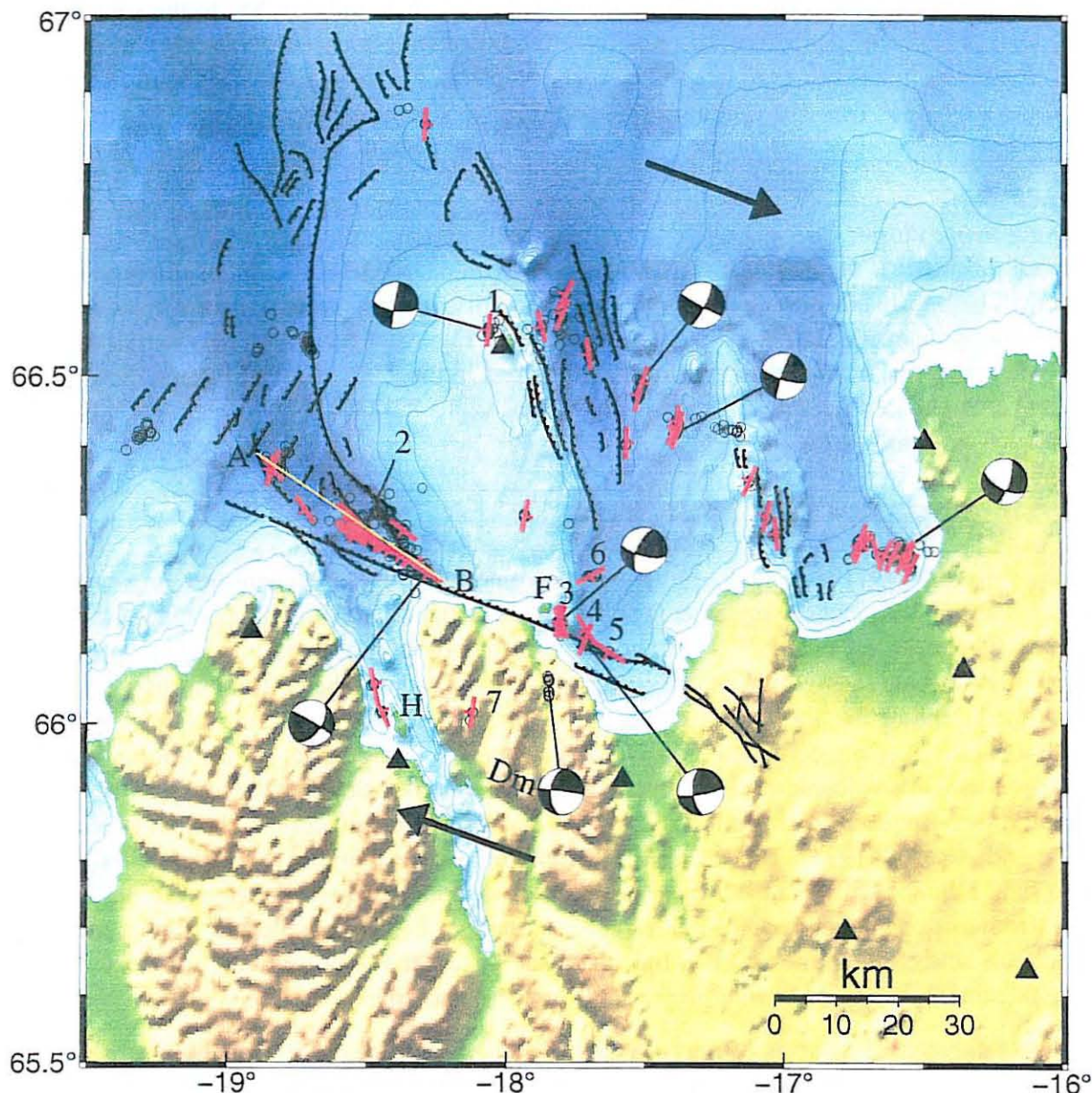


Figure 7. Mapped faults within the Tjörnes fracture zone. Black lines indicate faults mapped with conventional reflection seismic methods or by direct observations on-land. Red lines are 62 active fault segments mapped using accurate relative locations of microearthquakes. The fault plane solutions of selected earthquakes are shown on equal-area projections of the lower hemisphere. Seismic stations are denoted by filled triangles, earthquake epicenters after relocation by open circles. Dm is Dalsmynni valley, H and F are the islands Hrísey and Flatey, respectively. The yellow line between points A and B is the location of the vertical cross section in Figure 3. The arrows indicate the direction of plate motion (DeMets et al. 1990). The depth contour interval is 100 m. Within the Grímsey linement the faults strike approximately north-south. Movement on these faults is mostly left-lateral strike-slip. In the southwestern part, near the well-developed Húsavík-Flatey transform fault, there is a gradual change in the strike of active faults, from transform-parallel to ridge-parallel. Simultaneously the style of faulting changes from mostly right-lateral strike-slip on the transform parallel faults to more normal faulting on the ridge-parallel faults. The numbered groups (1-7) are discussed in the text.

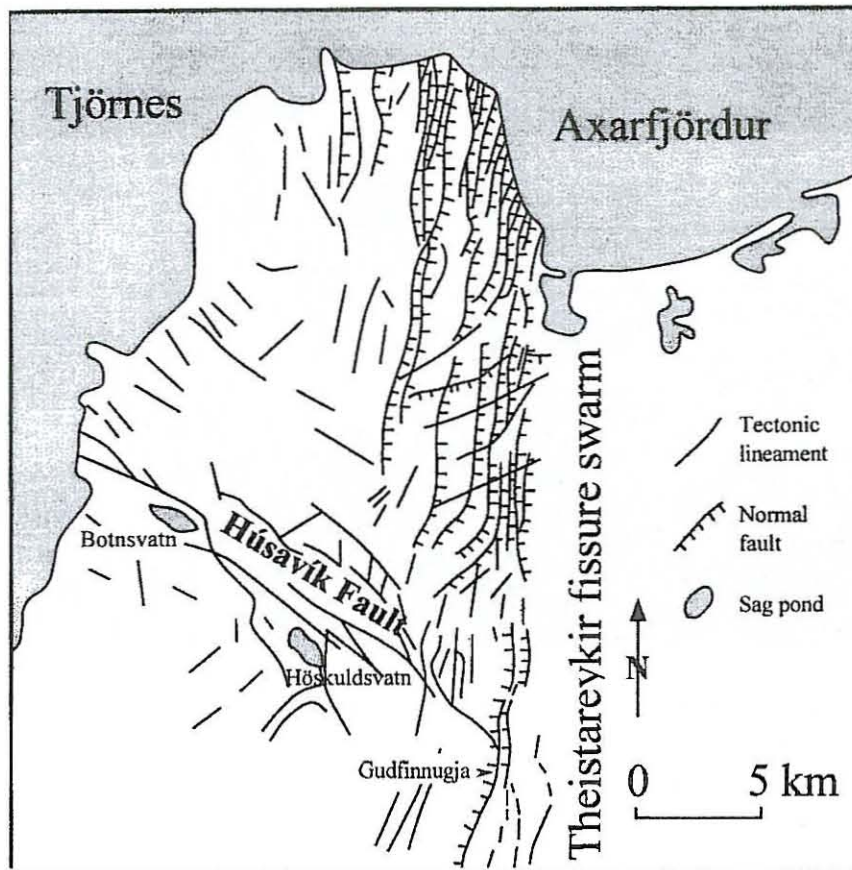


Figure 8. *General map of the Húsavík fault and the main normal faults and lineaments on the Tjörnes peninsula. The Húsavík fault meets with, and joins, normal faults of the Holocene Theistareykir fissure swarm in the active rift zone. The most clear-cut of these junctions occurs in a basaltic pahoehoe lava flow where the Húsavík fault joins the normal fault Gudfinnugjá (Guðmundsson et al. 1993). The trace of the Húsavík fault is marked by sag ponds (pull-apart structures); lake Botnsvatn is shown in Figure 10.*

M = 6.4 earthquake occurred in Axarfjörður, at the junction between the off-shore extension of the Krafla volcanic system and the Grímsey lineament (Björnsson et al. 1977). The fault-plane solution for this event shows strike-slip on planes striking N32°E or N122°E (Einarsson 1987). The N122°E direction is similar to the trend of the seismic lineament and has usually been interpreted as the strike of the fault plane, implying right-lateral movement. However, a strike of N32°E is close to what we observe in the microearthquake data. We therefore suggest that the M = 6.4 earthquake originated on a NNE-trending left-lateral fault, which is also in agreement with observations of on-land surface rupture in the vicinity of the earthquake epicenter (Björnsson et al. 1977).

7 THE HÚSAVÍK-FLATEY FAULT

The Húsavík-Flatey fault is a right-lateral strike-slip fault with a cumulative displacement of as much as 60 km. The fault has been active for 7–9 million years (Guðmundsson et al. 1993). On the Tjörnes peninsula the fault consists of many large-scale strike-slip segments (Figure 8). The HFF can be traced from the coast just north of the town of Húsavík to the western margin of the



Figure 9. *Intensely deformed basaltic lava flows associated with the Húsavík fault on the western coast of Tjörnes (the exposure is where the fault trace meets the coast, see Figure 8). View ESE along the strike of the fault, the backpack provides a scale. The deformed rock is characterized by extensive secondary mineralization and numerous slickensided surfaces.*

Holocene rift zone, a distance of some 25 km. This part, referred to as the Húsavík fault, consists of en-echelon, dominantly left stepping right-lateral strike-slip fault segments (Figure 8). The westernmost part of the Húsavík fault is moderately to steeply dipping and separates Tertiary rocks north of the fault from Upper Pleistocene rocks south of it (Sæmundsson 1974). Further east compressional structures are common on the fault. Fault-related deformation occurs in a 100 m wide belt running parallel with the fault segments. This deformation belt is characterized by closely spaced veins and fractures.

On the western coast of the Tjörnes peninsula, the fault rock of the Húsavík fault is crushed and altered in a zone as wide as 300 m. This zone consists of cataclastic rocks ranging from crush-breccias to microbreccias (Figure 9). Hematite-coated minor fault planes are common, as well as veins of zeolites and calcite. Vertical displacement on the Húsavík fault is more than 200 m and may be as much as 1400 m (Guðmundsson et al. 1993). This displacement is partly explained by the fault being oblique-slip; partly by its dip-slip reactivation, due to extension across the fault.

Both extensional and compressional features, creating topographic lows and highs, respectively, are associated with the Húsavík fault. For example, the sag pond (pull-apart basin) Botnsvatn (Figure 8 and Figure 10) is attributable to dilational bend in the trace of the fault. When the fault trace steps to the right, crustal extension and the formation of normal faults and pull-apart basins occurs. When the fault trace steps to the left, the overlap that develops leads to crustal compression. As a consequence, vertical uplift occurs and pressure ridges are created. Uplifted terrain and pressure ridges are especially common along the eastern part of the Húsavík fault, in agreement with the left-stepping character of this part of the fault. The crustal compression

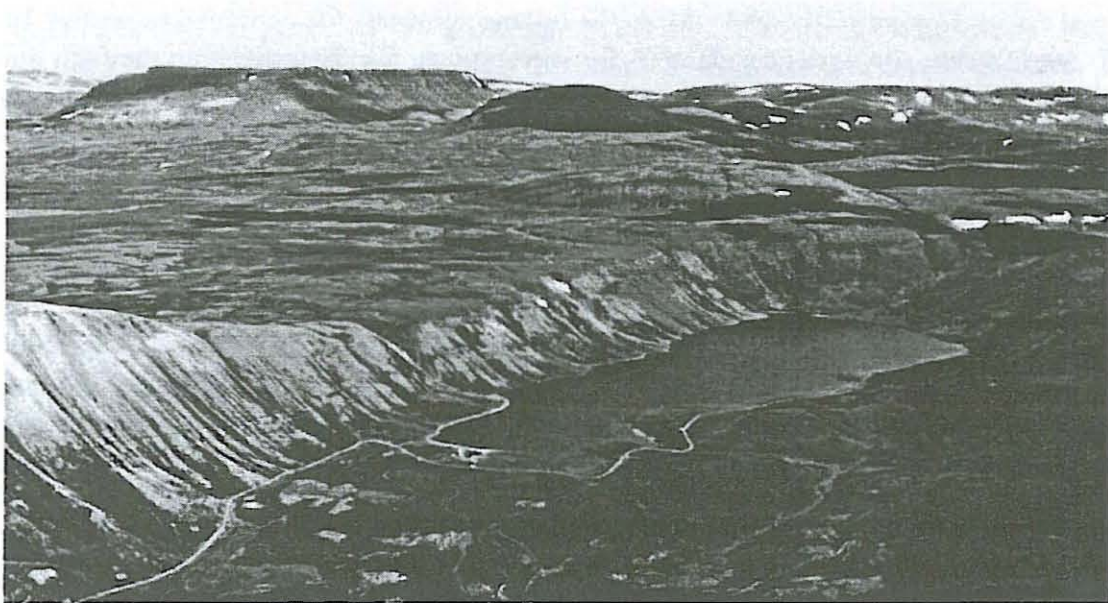


Figure 10. *Aerial view of Lake Botnsvatn, a sag pond associated with the Húsavík fault (for location see Figure 8). View NE, the fault scarp of the Húsavík fault reaches 200 m at the left margin of the photograph. The light color of the fault scarp is partly attributable to the numerous secondary minerals associated with the fault plane.*

indicates that some of the faults associated with the eastern part of the Húsavík fault may have a reverse component.

The main on-land exposure of the Húsavík-Flatey fault occurs on the northern coast of the Flateyjarskagi peninsula, where the fault is referred to as the Flatey fault. This part has been studied in detail by Jancin et al. (1985), Guðmundsson (1993) and Fjäder et al. (1994).

In recent years most of the earthquake activity near the HFF has taken place at two locations; near its western end where it joins the Kolbeinsey ridge, and some 40 km further east, where the HFF intersects the east flank of the Grímsey shoal platform. Fault planes estimated from accurate relative locations of earthquakes near the western end of the Húsavík-Flatey fault strike between N113°E and N146°E and dip 72°–90°, comparable to the strike and dip of the fault zone itself. The slip is mostly right-lateral, in agreement with field observations. As the transform fault joins the spreading ridge further west, the strike of mapped faults becomes more northerly (Figure 7). The faulting giving rise to microearthquakes also changes from right-lateral strike-slip at or close to the transform fault, to more normal faulting near the Kolbeinsey ridge.

Most of the active faults that we have mapped with earthquake data near the HFF east of the island of Flatey have northerly strikes, in contrast with the WNW strike of the transform fault itself (Figure 7). We used earthquakes from three separate clusters (labelled 3, 4 and 5 in Figure 7), one of which was divided into three subgroups, to obtain five estimates of strike directions at the three different locations. The four fault planes estimated from clusters 3 and 4 strike between N22°W and N23°E. Both clusters are on the eastern flank of the Grímsey shoal platform, just north of its intersection with the HFF. The strikes of the mapped faults are subparallel to the flank. Further north several flank-parallel faults have been observed in seismic profiles (McMaster et al. 1977). These faults can be traced from about 20 km north of the HFF for more than 30 km and appear to terminate near the island of Grímsey. They were interpreted

as normal faults dipping to the east. Most fault-plane solutions for earthquakes on the flank are left-lateral strike-slip with considerable dip-slip components. Extrapolating the fault plane solutions of the microearthquakes to the accumulated slip on the flank faults, the total horizontal movement on these faults may be two or three times greater than the vertical displacement.

The third swarm (labelled 5 in Figure 7) is located further east than the other two, close to the inferred location of the Húsavík-Flatey fault. This small swarm consists of six events that occurred on July 28, 1997. The strike of a plane defined by the relocated hypocenters is poorly constrained but the best fitting plane through the events strikes N123°E and dips 89° SW. We therefore associate this swarm with faulting on the HFF itself. This is the only earthquake cluster that has occurred on the HFF east of approximately longitude 18.3°W since the installation of the new seismic network in December 1993. Individual earthquakes on the eastern part of the HFF have also been few (Figure 1). Presumably the Krafla rifting episode 1975–1984 increased normal stress on the eastern part of the HFF and the shear stress that may have concentrated on the HFF due to the episode favored left-lateral movement rather than right-lateral movement. Thus, the Krafla rifting episode resulted in reduced earthquake activity on the eastern part of the fault. The small July 1997 earthquake swarm may signal the reactivation of the fault's eastern end.

Cluster 6 in Figure 7 is also located on the flank, about 10 km north of the Húsavík-Flatey fault. These earthquakes appear to occur on a plane striking N61°E and dipping 82° to the SSE. Faulting in this sequence was left-lateral strike-slip.

8 THE DALVÍK LINEAMENT

The third main seismic lineament in the TFZ is the Dalvík lineament, running parallel with, but located roughly 30 km south of, the Húsavík-Flatey fault (Figure 1). One of the basic structural elements supposed to support the Dalvík lineament being a WNW-trending strike-slip fault is the valley referred to as Dalsmynni (Figure 7). A systematic search for evidence of a WNW-trending strike-slip fault along this valley was made by the authors, but none were found. The northwestern channel of the main river in the valley is a deep canyon dissected into a Tertiary basaltic lava pile. Many basaltic dikes can be traced across the canyon without any strike-slip offset. No evidence exists for any large-scale faulting in the canyon that could be related to a major WNW-trending strike-slip fault. There are some minor faults (displacements of the order of centimeters or less) in the lavas inside and surrounding the canyon, and although some of these strike WNW, the dominant strike is N-S. The Dalsmynni valley, formed by glacier erosion, is presumably related to a major flexure zone that occurs in this area and offers a structural weakness in the basaltic lava pile (Jancin et al. 1985; Fjäder et al. 1994).

A systematic search for WNW-trending major faults has also been made on the west coast of the fjord Eyjafjörður, in the vicinity of the town of Dalvík (Figure 1) but none were found (Långbacka and Guðmundsson 1995). There are abundant fault planes in the vicinity of the town, but most of those have a northerly trend and are interpreted as left-lateral strike-slip faults. A sinistral strike-slip fault striking northnorthwest and having 20 m of cumulative slip has been reported on the island Hrísey (H in Figure 7) in Eyjafjörður (Friðleifsson 1989).

In the last few years, the Dalvík lineament has been much less active than the Húsavík-Flatey fault and the Grímsey lineament (Figure 1). Only three clusters of earthquakes have been recorded there since the installation of the new digital network. Due to the paucity of earthquake data from the Dalvík lineament we relaxed the requirement that each swarm should last

less than three days, imposed on data from other parts of the TFZ, and included one group (labelled 7 in Figure 7) that occurred during a period of ten days. Relocations of the earthquakes show faulting on northerly striking planes, rather than on a fault plane parallel to the trend of the lineament. The results suggest that faulting in the Dalvík lineament is similar to that observed in the Grímsey lineament, i.e. left-lateral strike-slip on several northerly trending faults, rather than right-lateral strike-slip on one or more faults parallel to the trend of the seismic lineament.

Considerable historical seismic activity is associated with the Dalvík lineament. The largest earthquake in the TFZ in recent decades, a $M = 7$ earthquake at the mouth of fjord Skagafjörður in 1963, occurred near the western end of the lineament. Fault-plane solutions for the 1963 earthquake were interpreted either as showing left-lateral movement on a N-S fault (Stefánsson 1966) or as right-lateral strike-slip on an E-W trending fault (Sykes 1967). The last major earthquake in the eastern part of the lineament was the $M = 6.3$ earthquake in 1934, near the town of Dalvík. We consider it likely that the Dalvík 1934 earthquake occurred on some of the north-trending left-lateral faults observed in the vicinity of the epicenter, a proposal that is also in agreement with the observed northward propagation of the rupture zones during the earthquake (Långbacka and Guðmundsson 1995), and the microseismicity data presented here.

9 DISCUSSION AND CONCLUSIONS

This study demonstrates that the use of relative locations of similar events is a very promising method for subsurface mapping of faults. By combinations with fault plane solutions the results can be independently checked. In particular, the accurate relative locations can distinguish between the true fault plane and the auxiliary plane. The peak slip in a magnitude 3 event is of the order of 1 cm and the radius of the rupture area a few hundred meters. This is comparable to the smallest displacements we measured in the field. The time window of the seismological data we use is less than four years, while the geological observations chronicle fault movements in the TFZ for the past 7–9 million years. Where both types of data are available, the seismological and geological observations agree very well.

The accurate relative locations of microearthquakes and detailed geological mapping show a distinct difference between the style of faulting near the Húsavík-Flatey fault and in the seismic lineaments north and south of the fault. The HFF is a well developed right-lateral transform fault where several tens of kilometers of horizontal displacement has occurred during the past 7–9 million years. Most of the faults that we have studied in the vicinity of the transform are oriented subparallel to the transform. The only exceptions are the earthquakes near Flatey island that appear to occur on N-S faults associated with the flank of the Grímsey shoal platform. In contrast with faulting on the HFF, faulting in the Grímsey and Dalvík lineaments is left-lateral on faults oriented at high angles to the overall trend of these lineaments.

Ridge-perpendicular (uniaxial) tensile loading (plate pull) is a permanent feature of the rift zones and leads to the development of a zone of high shear-stress concentration between the nearby ends of the rift zones (Pollard and Aydin 1984; Guðmundsson et al. 1993). However, this stress field cannot account for the transform-parallel extension fractures (dikes, normal faults) of the HFF, nor the curved fabric at the ridge-transform junction. Biaxial tensile loading, however, generates a stress field that can account for most of the observed structures of the Tjörnes fracture zone (Guðmundsson 1993, 1995a,b; Långbacka and Guðmundsson 1995) as well as the left-lateral strike-slip faults north and south of the HFF revealed by the microearthquakes.

The N trending left-lateral faults in the Tjörnes fracture zone form a conjugate system with the

WNW trending right-lateral faults that form the main part of the HFF (Guðmundsson 1993; Fjäder et al. 1994). Such conjugate systems are almost invariably generated in rock-fracture experiments (e.g. Farmer 1983) and are commonly found in seismic zones, e.g. the SISZ. In the SISZ the current seismicity is mainly associated with a conjugate system of NNE trending (mostly) right-lateral faults and ENE trending (mostly) left-lateral faults. These conjugate faults have also been identified in the field in the SISZ, both as minor faults (Angelier et al. 1996; Passerini et al. 1997) and as large-scale faults (Bjarnason et al. 1993; Guðmundsson 1995a; Luxey et al. 1997). The style of faulting in the SISZ thus appears similar to the faulting we observe in the Grímsey lineament. Both zones are relatively young, created in response to the propagation of rifting in the eastern and northern rift zones, respectively, and faulting occurs mostly on faults oriented at high angles to the trends of the seismic lineaments.

The NRZ north of the HFF has been propagating to the north for the past 1–2 million years. It follows that the N trending left-lateral faults in the TFZ are at least that old, and some of them may be as old as the HFF itself. Block rotation does not seem to be a viable mechanism to explain these N trending faults, as they would then have rotated out of their current trends a long time ago. We prefer to explain them in rock-mechanics terms as an ordinary, stable conjugate system to the right-lateral faults of the HFF. Comparison of the field data from the HFF and the current seismicity indicate that the controlling stress field has been broadly maintained throughout the history of that fault. The pre-existing structural grain of the area was presumably dominantly N-S oriented, i.e. N-S trending tension fractures and normal faults generated in the N-S trending rift zone. We propose that the propagation of the rift zone north of the HFF has increased the activity on, and presumably the number of, the N trending left-lateral faults, but our data indicate that this conjugate system and the associated stress field of the TFZ have been largely maintained during the development of the TFZ. When more of the transform motion becomes accommodated by the Grímsey lineament, the crustal segment occupied by this lineament becomes increasingly fractured and the associated stress field may change to one favoring transform-parallel faulting. Continued propagation of the NRZ to the north may eventually lead to the extinction of the HFF and the Dalvík lineament. According to this hypothesis, the Dalvík lineament is the remnants of a transform that never evolved past the initial stage of transform-perpendicular faulting. Before the Dalvík lineament matured, the rift zone had propagated further north and the HFF had taken over as the main transform zone.

Another possible future evolution of the Tjörnes fracture zone is that the Kolbeinsey ridge propagates to the south and connects, through the Dalvík lineament, with the NRZ, while the northern tip of the NRZ propagates to the north and connects, through the Grímsey lineament, with the Kolbeinsey ridge. Then the HFF would be situated between overlapping spreading centers, in which case most of the spreading would no longer be accommodated by the HFF but rather by the Grímsey and Dalvík lineaments and their potential future extensions. While this scenario is quite possible and, we think, not unlikely, our data do not allow us to elaborate this model at this stage.

Acknowledgments

Árni Vésteinsson at the Icelandic Hydrographic Service provided high resolution bathymetry data for parts of the TFZ. Most of the figures in this article were generated with the public domain GMT software (Wessel and Smith 1991). Financial support was provided by the Icelandic Research Council, grant 95–N–701, and by European Commission Environment and Climate Programme, contract ENV4–CT96–0252.

10 REFERENCES

- Angelier, J., S.Th. Rögnvaldsson, F. Bergerat, Á. Guðmundsson, S. Jakobsdóttir and R. Stefánsson 1996. Earthquake focal mechanisms and recent faulting: a seismotectonic analysis in the Vörðufell area, South Iceland seismic zone. In: B. Þorkelsson (editor), *Seismology in Europe*. Papers presented at the XXV ESC General Assembly, Reykjavík, Iceland, September 9–14, 1996. ISBN-9979-60-235-X, 199–204.
- Bjarnason, I., P. Cowie, M.H. Anders, L. Seeber and C.H. Scholz 1993. The 1912 Iceland earthquake rupture: growth and development of a nascent transform system. *Bull. Seism. Soc. Am.* 83, 416–435.
- Björnsson, A., K. Sæmundsson, P. Einarsson, E. Tryggvason and K. Grönvold 1977. Current rifting episode in North Iceland. *Nature* 266, 318–323.
- Böðvarsson, R., S.Th. Rögnvaldsson, S.S. Jakobsdóttir, R. Slunga and R. Stefánsson 1996. The SIL data acquisition and monitoring system. *Seism. Res. Lett.* 67, 35–46.
- Console, R. and R.D. Giovambattista 1987. Local earthquake relative location by digital records. *Phys. Earth Planet. Inter.* 47, 43–49.
- Deichmann, N. and M. Garcia-Fernandez 1992. Rupture geometry from high-precision relative hypocenter locations of microearthquake clusters. *Geophys. J. Int.* 110, 501–517.
- DeMets, C., R.G. Gordon, D.F. Argus and S. Stein 1990. Current plate motions. *Geophys. J. Int.* 101, 425–478.
- Einarsson, P. 1987. Compilation of earthquake fault plane solutions in the North Atlantic and Arctic oceans. In: K. Kasahara (editor), Recent plate movements and deformation. *Geodynamic series* 20, 47–62.
- Farmer, I. 1983. *Engineering behaviour of rocks*. Chapman and Hall, London.
- Fjäder, K., Á. Guðmundsson and T. Forslund 1994. Dikes, minor faults and mineral veins associated with a transform fault in North Iceland. *J. Struct. Geol.* 16, 109–119.
- Flóvenz, Ó.G. and K. Gunnarsson 1991. Seismic crustal structure in Iceland and surrounding area. *Tectonophysics* 189, 1–17.
- Fox, P.J. and D.G. Gallo 1986. The geology of North American plate boundaries and their aseismic extensions. In: P.R. Vogt and B.E. Tucholke (editors), *The geology of North America; the western North Atlantic region*. Geological Society of America, Boulder, Colorado, vol. M, 157–172.
- Frémont, M.J. and S. Malone 1987. High precision relative locations of earthquakes at Mount St. Helens, Washington. *J. Geophys. Res.* 92, 10223–10236.
- Friðleifsson, G.Ó. 1989. Jarðfræðipunktur um Hrísey 1989 (notes on the geology of Hrísey 1989). *Greinargerð Orkustofnunar GÓF/89-05*. Orkustofnun, Reykjavík. In Icelandic.
- Got, J.-L., J. Fréchet and F.W. Klein 1994. Deep fault plane geometry inferred from multiplet relative relocation beneath the south flank of Kilauea. *J. Geophys. Res.* 99, 15375–15386.
- Guðmundsson, Á. 1993. On the structure and formation of fracture zones. *Terra Nova* 5, 215–224.
- Guðmundsson, Á. 1995a. Ocean-ridge discontinuities in Iceland. *J. Geol. Soc. London* 152, 1011–1015.
- Guðmundsson, Á. 1995b. Stress fields associated with oceanic transform faults. *Earth Planet. Sci. Lett.* 136, 603–614.

- Guðmundsson, Á., S. Brynjólfsson and M.Þ. Jónsson 1993. Structural analysis of a transform fault–rift zone junction in North Iceland. *Tectonophysics* 220, 205–221.
- Ito, A. 1985. High resolution relative hypocenters of similar earthquakes by cross-spectral analysis method. *J. Phys. Earth* 33, 279–294.
- Jancin, M., K.D. Young, B. Voight, J.L. Aronson and K. Sæmundsson 1985. Stratigraphy and K/Ar ages across the west flank of the northeast Iceland axial rift zone, in relation to the 7 Ma volcano–tectonic reorganization of Iceland. *J. Geophys. Res.* 90, 9961–9985.
- Långbacka, B.O. and Á. Guðmundsson 1995. Extensional tectonics in the vicinity of a transform fault in North Iceland. *Tectonics* 14, 294–306.
- Luxey, P., P. Blondel and L.M. Parson 1997. Tectonic significance of the South Iceland transform zone. *J. Geophys. Res.* 102, 17967–17980.
- McMaster, R.L., J.-G.E. Schilling and P.R. Pinet 1977. Plate boundary within Tjörnes fracture zone on northern Iceland's insular margin. *Nature* 269, 663–668.
- Passerini, P., M. Marcucci, G. Sguazzoni and E. Pecchioni 1997. Longitudinal strike-slip faults in oceanic rifting: a mesostructural study from western to southeastern Iceland. *Tectonophysics* 269, 65–89.
- Pollard, D.D. and Y. Aydin 1984. Propagation and linkage of oceanic ridge segments. *J. Geophys. Res.* 89, 10017–10028.
- Rögnvaldsson, S.Th. and R. Slunga 1993. Routine fault plane solutions for local and regional networks: a test with synthetic data. *Bull. Seism. Soc. Am.* 11, 1247–1250.
- Rögnvaldsson, S.Th. and R. Slunga 1994. Single and joint fault plane solutions for microearthquakes in South Iceland. *Tectonophysics* 273, 73–86.
- Slunga, R. 1981. Earthquake source mechanism determination by use of body–wave amplitudes - an application to Swedish earthquakes. *Bull. Seism. Soc. Am.* 71, 25–35.
- Slunga, R., P. Norrmann and A.-C. Glans 1984. Baltic shield seismicity, the results of a regional network. *Geophys. Res. Lett.* 11, 1247–1250.
- Slunga, R., S.Th. Rögnvaldsson and R. Böðvarsson 1995. Absolute and relative location of similar events with application to microearthquakes in southern Iceland. *Geophys. J. Int.* 123, 409–419.
- Sæmundsson, K. 1974. Evolution of the axial rifting zone in northern Iceland and the Tjörnes fracture zone. *Geol. Soc. Am. Bull.* 85, 495–504.
- Sæmundsson, K. 1979. Outline of the geology of Iceland. *Jökull* 29, 7–21.
- Stefánsson, R. 1966. Methods of focal mechanism studies with application to two Atlantic earthquakes. *Tectonophysics* 3, 209–243.
- Stefánsson, R., R. Böðvarsson, R. Slunga, P. Einarsson, S. Jakobsdóttir, H. Bungum, S. Gregersen, J. Havskov, J. Hjelme and H. Korhonen 1993. Earthquake prediction research in the South Iceland seismic zone and the SIL project. *Bull. Seism. Soc. Am.* 83, 696–716.
- Sykes, L.R. 1967. Mechanism of earthquakes and nature of faulting on the mid–oceanic ridges. *J. Geophys. Res.* 72, 2131–2153.
- Tryggvason, A. 1998. *Seismic tomography: inversion for P- and S-wave velocities*. Ph.D. thesis, Uppsala University, Uppsala, Sweden.
- Tryggvason, E. 1973. Seismicity, earthquake swarms, and plate boundaries in the Iceland re-

gion. *Bull. Seism. Soc. Am.* 63, 1327–1348.

Wessel, P. and W.H.F. Smith 1991. Free software helps map and display data. *EOS* 72, 441 and 445–446.

ISSN 1025-0565
ISBN 9979-878-11-8

Kápu mynd: Klósigar (vatnslær)
Ljós m.: Guðmundur Hafsteinsson, veðurfræðingur